Poisson's spot with molecules

Thomas Reisinger,[1,*] Amil A. Patel,[2] Herbert Reingruber,[3] Katrin Fladischer,[3] Wolfgang E. Ernst,[3] Gianangelo Bracco,[4] Henry I. Smith,[2] and Bodil Holst[1]

[1]*Department of Physics and Technology, University of Bergen, Allégaten 55, 5007 Bergen, Norway*
[2]*NanoStructures Laboratory, Massachusetts Institute of Technology, Cambridge, Massachusetts 02139, USA*
[3]*Institute of Experimental Physics, Graz University of Technology, Petersgasse 16, 8010 Graz, Austria*
[4]*Department of Physics and CNR-IMEM, University of Genova, V. Dodecaneso 33, 16146 Genova, Italy*

In the Poisson-spot experiment, waves emanating from a source are blocked by a circular obstacle. Due to their positive on-axis interference an image of the source (the Poisson spot) is observed within the geometrical shadow of the obstacle. In this paper we report the observation of Poisson's spot using a beam of neutral deuterium molecules. The wavelength independence and the weak constraints on angular alignment and position of the circular obstacle make Poisson's spot a promising candidate for applications ranging from the study of large molecule diffraction to patterning with molecules.

　　　　PACS number(s): 37.20.+j, 03.75.−b, 37.25.+k

Diffraction experiments played a crucial role in establishing the existence of de Broglie matter waves [1–3]. Today, matter-wave diffraction is used, among other applications, to investigate quantum interference of large molecules [4], enabling the study of quantum decoherence [5] and its role in the quantum-to-macroscopic-world transition. These experiments have mostly been carried out with free-standing material gratings [6,7] or light wave gratings [8]. The largest molecules so far (>3 nm) for which quantum interference was successfully demonstrated were perfluoroalkyl-functionalized azobenzenes in a Kapitza-Dirac-Talbot-Lau interferometer [9]. Scaling such experiments to even larger objects, such as macromolecules or perhaps even viruses, is a tantalizing prospect. In principle, this should be possible to some degree with a Kapitza-Dirac-Talbot-Lau interferometer. However, as the size of the molecule and/or object approaches the distance between grating bars difficulties arise. In the case of material gratings, van der Waals (vdW) forces increasingly limit interference contrast by adding a locally varying coherent phase shift. In fact, even blocking may occur. In the case of light gratings spontaneous emission and photon absorption are likely to perturb coherence. Furthermore, for the Talbot-Lau configuration the distance between the three gratings is a function of wavelength, and thus requires wavelength selection. This limits effective intensity of the commonly used thermal sources because only a fraction of the emitted molecules can be used in the experiment. In the case of clusters, the necessity of mass selection constrains effective source intensity additionally. Finally, alignment of the gratings, both with respect to each other and the vertical, is challenging, and misalignment can cause classical Moiré fringes which differ from expected interference patterns only in visibility and wavelength dependence.

In this paper we make use of the Poisson-spot configuration to demonstrate quantum interference in a beam of molecules. The Poisson spot refers to a classical-optics experiment, in which a point light-source is blocked by a circular obstacle. Wave theory predicts that the intensity on the optical axis within the geometrical shadow is the same as without the blocking obstacle due to the cylindrical symmetry [11], resulting in a bright interference spot, called the Poisson spot. When compared to the Talbot-Lau configuration, this setup reduces interaction with the diffracting structure to a single edge, limiting the impact of vdW forces and blocking is not an issue. In addition, the vdW influence can be reduced by creating free-standing structures from thinner membranes, perhaps even from two-dimensional (2D) crystals such as graphene. Furthermore, the on-axis interference condition giving rise to the Poisson spot is wavelength independent, which means that experiments can be carried out using a polychromatic source. Thus, the Poisson-spot configuration can utilize the entire mass and/or velocity spectrum of the beam source, which increases the available intensity at the detector. It also places only weak constraints on angular alignment and position of the circular obstacle [12]. These are important differences also when compared to diffraction experiments using Fresnel zone-plates [13,14], and make the Poisson spot an interesting option for studying the quantum-mechanical nature of molecules.

One-dimensional (1D) Fresnel diffraction has been demonstrated before by Mlynek *et al.* [15] in a wire interferometer using a beam of metastable helium. This configuration is, however, less suited to diffraction of larger objects since it can be shown that its ideal diffraction efficiency (diffracted intensity divided by intensity of undisturbed beam from a point source) diminishes with decreasing wavelength. In comparison, the on-axis diffraction efficiency for the Poisson-spot configuration is unity for a point source, regardless of wavelength. Furthermore, the wire setup's scalability is dependent on an efficient line detector, while the cylindrical symmetry of the Poisson spot is more suited to a point-like detector, which is simpler to implement. Recent advances in field-ionization molecular-beam detectors promise highly efficient point detectors [16].

The original Poisson spot experiment played a crucial role in proving the wave nature of light. At the beginning of the 19th century evidence for the wave nature of light was accumulating (Young's double-slit experiment [17] was published
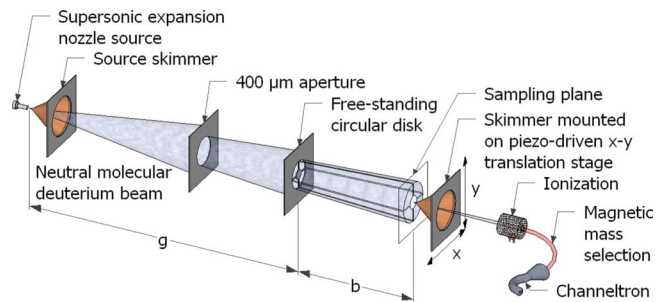
---

*treisinger@gmail.com

FIG. 1. (Color online). Poisson-spot experimental setup: A beam of neutral D_2 is created in a supersonic expansion from a 10 μm nozzle at 11 bar source pressure, and cooled with liquid nitrogen to a temperature of 101 K. This results in a terminal beam velocity of $v = 1060$ ms^{-1}, as determined from time-of-flight spectra, corresponding to a de Broglie wavelength of $\lambda = 0.096$ nm. The measured velocity spread is $\Delta v / v = 0.054$. The source size is defined by the 50 μm-diameter source skimmer made from a glass pipette [10]. A shadow is cast by a free-standing circular disk of 60 μm diameter located at $g = 1496$ mm and sampled at distances $b = 321$, 641, and 801 mm using an 11 μm-aperture skimmer (prevents back streaming) mounted on an *x-y* piezo table. An electron-bombardment ionization region together with a magnetic sector for mass selection and a channeltron are used for detection of the beam.

in 1807), but the corpuscular theory of Isaac Newton [18] still had many supporters. In 1818 the French Academy launched a competition to explain the properties of light. Augustin Fresnel entered the competition by submitting his wave theory of light [19]. One of the members of the judging
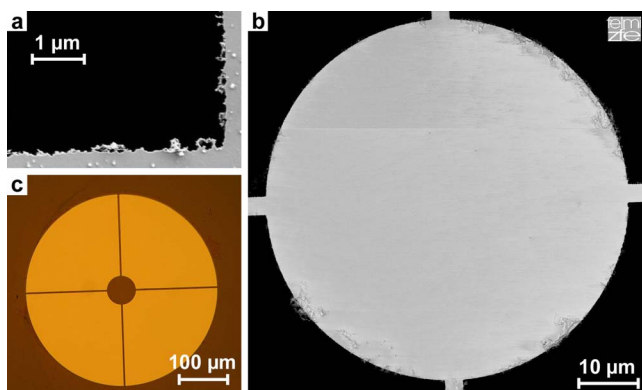

FIG. 2. (Color online). Electron and optical microscopy images of the circular obstacle. It is a free-standing silicon nitride (SiN_x) disk, 60 μm in diameter, less than 1 μm in thickness and suspended by four narrow support bars. It was fabricated at the Nano-Structures Laboratory of MIT. The pattern was written by scanning-electron-beam lithography and transferred into the SiN_x using reactive-ion etching. (a) The scanning-electron micrograph shows the edge of the free-standing circular disk at the corner of the left-most support bar in the same orientation as in the larger scale micrographs. The edge roughness is close to minimal there and measures about 250 nm peak-to-peak. The scanning-electron micrograph in (b) reveals additional edge roughness in the form of remnants from etching protruding up to 500 nm from the disk edge. (c) Optical micrograph showing the outer aperture of 400 μm diameter.
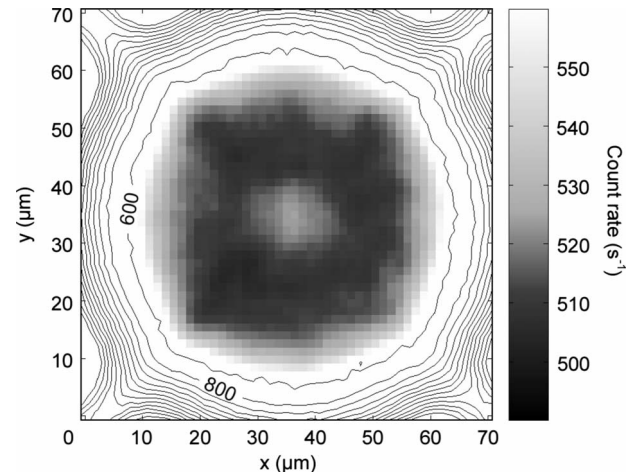

FIG. 3. 2D image of a molecular-beam Poisson spot. The contour lines show the higher intensity regions along the edge of the shadow, revealing the positions of the support bars. They are separated by 200 counts per second. The central part of the shadow is amplified as a grayscale image plot. The image is the sum of 24 images recorded consecutively at a sampling distance of 321 mm (2.8 h recording time per image). The images were summed with a variable pixel shift, determined from minimizing the sum of squared pixel-value differences. This was done to compensate for misalignment due to temperature drifts. A 2-by-2 Savitzky-Golay filter was applied to reduce noise.

committee was the great Siméon-Denis Poisson, a supporter of Newton's theory. Poisson showed that a consequence of Fresnel's theory was that there would exist an on-axis bright spot in the shadow of a circular obstacle. Poisson immediately concluded that this was an absurd result (as indeed it would have been if Newton's particle theory of light had been correct). However, the head of the committee, François-Jean-Dominique Arago decided to perform the experiment using a 2 mm metallic disk molded to a glass plate with wax [19]. He immediately observed the predicted spot and Fresnel won the competition. Arago later noted that the phenomenon (which was later to be known as Poisson's spot or the spot of Arago) had already been observed by Delisle [20] and Maraldi [21] a century earlier.

In this paper we present the first realization of a Poisson spot with molecules using a cold quasimonochromatic deuterium (D_2) beam. We favored a supersonic expansion beam because of its high brightness and low divergence, trading them for low detection efficiency (about 10^{-5}). The general setup is depicted in Fig. 1 and the circular obstacle in Fig. 2. A two-dimensional image of a D_2 Poisson spot is shown in Fig. 3. For a perfect point source the Poisson spot should reach the same intensity as outside the shadow, as predicted by Poisson. In fact, for plane waves (large source-to-obstacle distance) the on-axis intensity is expected to increase from zero, adjacent to the disk, to 90% of the unobstructed intensity only 1.5 diameters downstream of the circular obstacle, and the Poisson spot's full width half maximum is approximately given by $(b\lambda)/(r\pi)$, where r is the disk's radius [22]. In our experiment the intensity of the Poisson spot is decreased with respect to unobstructed intensity outside the shadow, mainly because of the limited transverse coherence
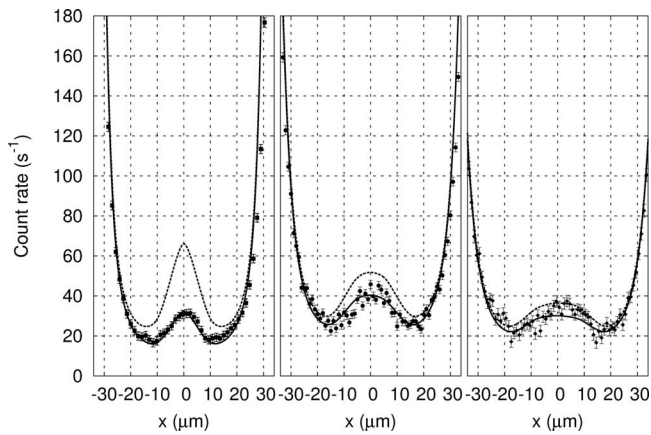
FIG. 4. The Poisson spot for three different disk-to-sampling plane distances: (a) 321 mm, (b) 641 mm, and (c) 801 mm. The data set in (a) is the horizontal profile of the image in Fig. 3 with an accumulated measurement time per data point of 136 s. The measurement time per data point was 120 s for the medium sampling distance and 60 s for the largest. The error bars show statistical uncertainty only. The unobstructed count rates were 3800 s^{-1}, 2500 s^{-1}, and 1700 s^{-1}, respectively, giving diffraction efficiencies of about 1%–2%. The lines show the result of model calculations, taking into account the actual measured unobstructed beam intensities. The dashed lines show the diffraction pattern to be expected from an ideally shaped circular disk, while the continuous lines show model results taking into account roughness, which was modeled by a fourth power sine with a period of about 1 μm and a peak-to-peak amplitude of 300 nm added to the edge of the ideal disk. Fitting the data to the calculation was achieved solely by subtracting background (approximately 475 s^{-1}) and adjusting for any lateral misalignment. When an edge corrugation of 300 nm is incorporated there is an excellent agreement between simulated and measured intensity profiles. This level of edge corrugation also corresponds very well to the observed defects (Fig. 2).

of the source, i.e., the finite source size given by the 50 μm-diameter source skimmer.

In Fig. 4 a series of one-dimensional plots show the intensity distribution across the Poisson spot for three different distances to the circular obstacle (distance b in Fig. 1). The experimental data is shown together with model calculations. The expected diffracted intensity profile was calculated in a two-step process: First, a 2D diffraction image is computed for a point source, applying an algorithm devised by Dauger [23]. The algorithm was adapted to take advantage of the radial symmetry of the problem. The outer aperture edge and support bars were neglected in all calculations. A variation in the disk radius was used to simulate roughness of the disk edge. In the second step the pattern to be expected from the extended source of the supersonic expansion is arrived at by incoherently summing contributions from a large number of independent point sources distributed randomly in the source plane. In this experiment the diameter of the extended source is simply the skimmer diameter. This can be deduced from previous results of experiments on the size of the virtual source in supersonic expansions [24]. The diffraction image of off-axis points is derived from the on-axis image by shifting it in the sampling plane, as deduced from the geometrical magnification $M=b/g$.

The two sets of model calculations shown in Fig. 4 correspond to a disk with (continuous line) and without (dashed lines) edge roughness, revealing its effect on the Poisson-spot intensity. At the closest distance considerable dampening may be noted while at the farthest position the difference to an ideal disk is less than the experimental uncertainty. The effect of disk edge roughness can be understood using the Fresnel zone concept [25]. The width Δr of the first Fresnel zone beyond the disk edge is given by $\Delta r \sim [r^2 + \lambda gb/(g+b)]^{0.5} - r$. In order for the Poisson-spot intensity to be solely determined by source coherence, edge roughness must be small compared to the adjacent Fresnel zone width or the wave front's positive interference is disturbed. Note that the further away from the circular obstacle the Poisson spot is observed, the larger the zones are, resulting in a smaller influence of a given edge roughness. This is in good agreement with our measurements.

The second effect to consider is the attractive vdW interaction between molecules and the disk, whose potential can be written in the form $V=-C_3/d^3$ where d is the distance between disk edge and molecule. The value $C_3 = 0.33$ meV nm^3 has been determined experimentally for the interaction between D_2 and SiN_x [26]. Crossing the force field, the molecules undergo a phase shift [27] and are deflected toward the disk edge. However, since the vdW interaction is weak and decays quickly with d, these two contributions are only important for molecules passing closer than 50 nm to the disk edge. The adjacent Fresnel zone is much wider so any phase shift in this region can be safely neglected. Further, the force field causes particles passing close to the disk edge to be deflected into the shadow. For an ideal circular disk this results in an on-axis intensity peak. However, as our model showed, this intensity is smeared out to less than measurement uncertainty by edge corrugation, which is large with respect to the 50-nm vdW interaction zone, and is therefore not shown in Fig. 4. The simulation of vdW forces was achieved by sampling molecular trajectories and calculating their deflection in the force field. To this end the field was assumed to be constant for each individual trajectory and restricted to the region of width equal to the disk's thickness.

Finally, we discuss briefly a few more potential applications of the Poisson-spot setup. A very interesting field of study could be the investigation of transverse coherence and aberrations of atom lasers [28,29] by measuring the deviation from a point-source Poisson-spot profile. The ideal coherence properties of a Bose-Einstein condensate (BEC) imply that the Poisson spot in the perfect case would be characterized by a Bessel-type beam profile. The Poisson spot could also be used for the deposition of large molecules on substrates with high lateral precision. This has many technological applications. Advances in, for example, self-assembly techniques or electron-beam-induced deposition have opened some possibilities. However, in the case of electron-beam-induced deposition the process tends to break up large molecules and in the case of self-assembly the technique is limited in terms of species and patterns. Poisson-spot-based "focusing" has the potential to become a nondestructive and species-independent patterning technique. It should be possible to create a "dot-matrix" printer setup, enabling fast and flexible patterning.

---

[1] L. de Broglie, Nature (London) **112**, 540 (1923).

[2] C. Davisson and L. Germer, Nature (London) **119**, 558 (1927).

[3] I. Estermann and O. Stern, Z. Phys. **61**, 95 (1930).

[4] M. Arndt, O. Nairz, J. Vos-Andreae, C. Keller, G. van der Zouw, and A. Zeilinger, Nature (London) **401**, 680 (1999).

[5] L. Hackermüller, K. Hornberger, B. Brezger, A. Zeilinger, and M. Arndt, Nature (London) **427**, 711 (2004).

[6] J. Schmiedmayer, M. S. Chapman, C. R. Ekstrom, T. D. Hammond, D. A. Kokorowski, A. Lenef, R. A. Rubenstein, E. T. Smith, and D. E. Pritchard, in *Atom Interferometry*, edited by P. R. Berman (Academic, San Diego, 1997), pp. 1–83.

[7] W. Schöllkopf and J. P. Toennies, Science **266**, 1345 (1994).

[8] E. M. Rasel, M. K. Oberthaler, H. Batelaan, J. Schmiedmayer, and A. Zeilinger, Phys. Rev. Lett. **75**, 2633 (1995).

[9] S. Gerlich, *et al.*, Nat. Phys. **3**, 711 (2007).

[10] J. Braun, P. K. Day, J. P. Toennies, G. Witte, and E. Neher, Rev. Sci. Instrum. **68**, 3001 (1997).

[11] J. J. Stamnes, *Waves in Focal Regions* (Hilger, Bristol, 1986).

[12] J. Coulson and G. G. Becknell, Phys. Rev. **20**, 594 (1922).

[13] R. B. Doak, R. E. Grisenti, S. Rehbein, G. Schmahl, J. P. Toennies, and C. Wöll, Phys. Rev. Lett. **83**, 4229 (1999).

[14] M. Koch, S. Rehbein, G. Schmahl, T. Reisinger, G. Bracco, W. E. Ernst, and B. Holst, J. Microsc. **229**, 1 (2008).

[15] S. Nowak, N. Stuhler, T. Pfau, and J. Mlynek, Phys. Rev. Lett. **81**, 5792 (1998).

[16] F. S. Patton, D. P. Deponte, G. S. Elliott, and S. D. Kevan, Phys. Rev. Lett. **97**, 013202 (2006).

[17] T. Young, *A Course of Lectures on Natural Philosophy and the Mechanical Arts* (Joseph Johnson, London, 1807).

[18] I. Newton, *Opticks: Or, A Treatise of the Reflections, Refractions, Inflections and Colours of Light* (Royal Society, London, 1704).

[19] A. J. Fresnel, *OEuvres Completes 1* (Imprimerie impériale, Paris, 1868).

[20] J.-N. Delisle, in Mémoires de l'Académie Royale des Sciences, 166 (1715).

[21] G. F. Maraldi, in Mémoires de l'Académie Royale des Sciences, 111 (1723).

[22] J. E. Harvey and J. L. Forgham, Am. J. Phys. **52**, 243 (1984).

[23] D. E. Dauger, Comput. Phys. **10**, 591 (1996).

[24] T. Reisinger, G. Bracco, S. Rehbein, G. Schmahl, W. E. Ernst, and B. Holst, J. Phys. Chem. A **111**, 12620 (2007).

[25] M. Born and E. Wolf, *Principles of Optics* (Cambridge University Press, Cambridge, 1999).

[26] R. E. Grisenti, W. Schollkopf, J. P. Toennies, G. C. Hergerfeldt, and T. Kohler, Phys. Rev. Lett. **83**, 1755 (1999).

[27] J. D. Perreault, A. D. Cronin, and T. A. Savas, Phys. Rev. A **71**, 053612 (2005).

[28] K. B. Davis, M. O. Mewes, M. R. Andrews, N. J. van Druten, D. S. Durfee, D. M. Kurn, and W. Ketterle, Phys. Rev. Lett. **75**, 3969 (1995).

[29] G.-B. Jo, J.-H. Choi, C. A. Christensen, Y.-R. Lee, T. A. Pasquini, W. Ketterle, and D. E. Pritchard, Phys. Rev. Lett. **99**, 240406 (2007).